

# Shear strength of reinforced concrete columns with five-spiral reinforcement

Yu-Chen Ou<sup>a</sup>, Jhe-Yan Li<sup>b</sup>, Hwasung Roh<sup>c,\*</sup>

<sup>a</sup> Department of Civil Engineering, National Taiwan University, Taipei, Taiwan

<sup>b</sup> Department of Civil Engineering, National Taiwan University, Taipei, Taiwan

<sup>c</sup> Department of Civil Engineering & Research Institute for Disaster Prevention, Jeonbuk National University, Jeonju, Republic of Korea

## ARTICLE INFO

### Keywords:

Shear strength  
Five-spiral reinforcement  
Columns  
Discrete computational shear strength model (DCSS)  
Seismic  
Cyclic

## ABSTRACT

Five-spiral transverse reinforcement for square reinforced concrete columns has been proven to possess a confinement capability superior to that of conventional rectilinear tie reinforcement. The objective of this research is to investigate the shear capacity of five-spiral reinforcement. Large-scale shear-critical five-spiral columns and comparable conventional tied columns were tested using double-curvature lateral cyclic loading. Test results showed that with the same amount and similar yield strengths of shear reinforcement and concrete compressive strengths, the column with five-spiral reinforcement exhibited a slightly lower shear strength than the counterpart tied column. All the five-spiral columns showed a lower speed of strength degradation after the peak load than counterpart tied columns. Failure of the five-spiral column under a high axial load was caused by fracture of the spirals. In contrast, failure of the rectilinear tie reinforcement was caused by premature failure of the hook anchorage. A modified Discrete Computational Shear Strength (DCSS) model was developed in this research for calculating the shear strength of five-spiral reinforcement. Comparison with the test results showed that the modified DCSS model provides conservative estimation of shear strength contributed by five-spiral reinforcement. Moreover, the DCSS model provides a degree of conservatism similar to the code equation for tie reinforcement.

## 1. Introduction

Spiral reinforcement is more effective in providing confinement to concrete than rectilinear tie reinforcement. Spiral reinforcement can resist concrete expansion at every location along the spiral while rectilinear reinforcement is only effective at bends. Spiral columns showed excellent performance during previous extreme events such large earthquakes (e.g. Murphy [1]) and blast and impact loadings (e.g. Mlakar et al. [2]). Spiral reinforcement fits well to columns with a circular cross section. To use spiral reinforcement in columns with other cross sections, multi-spiral reinforcement has been developed, including two-spiral reinforcement [3–8] and seven-spiral reinforcement [9–11] for oblong columns, five-spiral reinforcement [12–13] for square columns, and six-spiral reinforcement [14] and eleven-spiral reinforcement [10] for rectangular columns. This research focuses on the five-spiral reinforcement, which is illustrated in Fig. 1.

The five-spiral reinforcement consists of a central large spiral and four small spirals at the four corners of the column. The four small

spirals are used to increase the area of confined concrete around the four corners of the column. Fig. 1(a) shows the five-spiral reinforcement tested earlier in the studies presented in Yin et al. [12] and Yin et al. [13]. Fig. 1(b) shows the five-spiral reinforcement developed later [15] and studied in this research. Compared with the previous design, the central large spiral is increased to maximize the confined area. Tests on columns with the new design were conducted to investigate the axial compressive behavior of columns with five-spiral reinforcement [15]. It was found that columns with five-spiral reinforcement even with a smaller amount still showed better strength and ductility than those with conventional rectilinear tie reinforcement. To ensure interlocking between the small and large spirals, it is suggested that the maximum distance between the inner faces of small and large spirals in the overlapping region should be at least equal to the smaller value of 0.3 times the inner diameter of the small spiral and 60 mm. This suggestion has been added to the reinforced concrete code of Taiwan [16]. Moreover, the size of the small spiral can be taken approximately 0.3 times the size of the large spiral. A larger size of the small spiral does not significantly increase the performance of the column [15].

\* Corresponding author.

E-mail address: [hwasung@jbnu.ac.kr](mailto:hwasung@jbnu.ac.kr) (H. Roh).

<https://doi.org/10.1016/j.engstruct.2021.111929>

Received 26 May 2020; Received in revised form 15 December 2020; Accepted 15 January 2021

Available online 5 February 2021

0141-0296/© 2021 Elsevier Ltd. All rights reserved.

Notations	
$A_{bt}$	area of an individual transverse reinforcement
$A_{ch}$	cross-sectional area measured to the outside edges of transverse reinforcement
$A_g$	gross area of concrete cross section
$A_v$	area of shear reinforcement within spacings
$b_w$	web width
$d$	distance from extreme compression fiber to centroid of longitudinal tension reinforcement
$D_j$	diameter of $j$ -th spiral
$D_L$	diameter of large spiral
$D'_L$	outside diameter of large spiral
$D_S$	diameter of small spiral
$D'_S$	outside diameter of small spiral
$D''_S$	inside diameter of small spiral
$f'_c$	specified compressive strength of concrete
$f'_{ca}$	actual compressive strength of concrete
$f_{yt}$	specified yield strength of transverse reinforcement
$f_{yta}$	actual yield strength of transverse reinforcement
$f_{yl}$	specified yield strength of longitudinal reinforcement
$f_{yla}$	actual yield strength of longitudinal reinforcement
$h$	overall depth of section
$\ell_j$	length measured from the origin of coordinate to left edge of $j$ -th spiral
$\ell_c$	length measured from the origin of coordinate to left edge of column
$M_n$	nominal flexural strength
$N_u$	applied axial compressional force for equation of $V_c$
$P$	applied axial compressional force
$R_j$	radius of $j$ -th spiral
$R_L$	radius of large spiral
$R_S$	radius of small spiral
$s$	spacing of shear reinforcement
$V_c$	shear strength provided by concrete
$V_j$	shear strength provided by $j$ -th spiral
$V_{M_n}$	shear corresponding to nominal moment strength
$V_n$	nominal shear strength
$V_{n,Code}$	nominal shear strength computed by ACI318 code
$V_{n,DCSSm}$	nominal shear strength computed by modified DCSS model
$V_{n,DCSS}$	nominal shear strength computed by original DCSS model
$V_s$	nominal shear strength provided by shear reinforcement
$V'_s$	shear strength provided by each spiral with chosen origin of Cartesian coordinate system
$V_{s,Code}$	shear reinforcement strength computed by Eq.15
$V_{s,DCSSm}$	shear reinforcement strength computed by modified DCSS method
$V_{s,DCSS}$	shear reinforcement strength computed by DCSS method
$V_{test}$	maximum lateral force obtained from experiment
$x_i$	$x$ -coordinate of intersection of shear crack and $i$ -th layer of spiral equation
$x_i^1$	$x_i$ of the first intersection as shown in Fig. 9
$x_i^2$	$x_i$ of the second intersection as shown in Fig. 9
$\alpha_i$	angle between horizontal line passing center of spiral to point intersected by shear crack for $i$ -th intersection
$\alpha_i^1$	$\alpha_i$ of the first intersection as shown in Fig. 9
$\alpha_i^2$	$\alpha_i$ of the second intersection as shown in Fig. 9
$\beta_L$	angle between longitudinal axis of column and large spiral equation from elevation view
$\beta_S$	angle between longitudinal axis of column and small spiral equation from elevation view
$\theta$	angle between shear crack and longitudinal direction of column
$\rho_g$	ratio of longitudinal reinforcement area to gross area
$\rho_s$	volumetric ratio of transverse reinforcement
$\phi_b$	proportion of spiral bounded between section width limitation

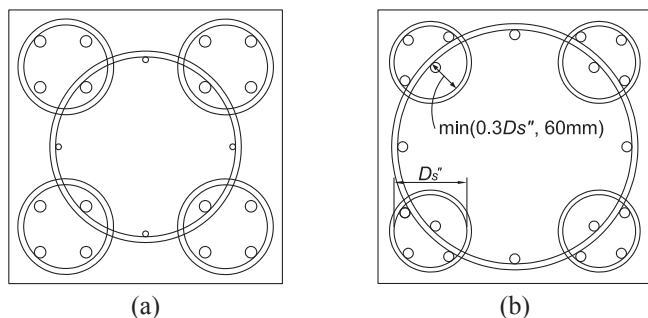


Fig. 1. Five-spiral reinforcement: (a) tested in Yin et al. [12] and Yin et al. [13]; (b) tested in this research.

Regarding the required amount of five-spiral reinforcement for the plastic hinge region of columns of special moment frames resisting earthquake forces, it is proposed [12] that the volumetric ratio of each spiral of five-spiral reinforcement should not be less than that required by the ACI 318 code [17] for spiral transverse reinforcement. The area  $A_{ch}$  used to calculate the required volumetric ratio is measured to the outside edges of all the spirals. This proposal has been added to the reinforced concrete code of Taiwan [16].

The objective of this research is to investigate the shear behavior of reinforced concrete columns with five-spiral reinforcement, which has

never been studied before. Large-scale shear-critical columns with five-spiral reinforcement were tested in this research using lateral cyclic loading. Counterpart columns with conventional rectilinear tie reinforcement were also tested. Test results were used to investigate the shear behavior of five-spiral columns and to develop the shear strength model for five-spiral reinforcement.

## 2. Experimental program

### 2.1. Specimen design and test setup

Four large-scale square columns were designed and tested in this research. The design parameters and material strengths are listed in Table 1. The dimension and reinforcement design of the columns are illustrated in Fig. 2. Two columns, designated as Y1S and Y3S, were designed with five-spiral reinforcement and the other two, designated as R1S and R3S, were designed with conventional rectilinear tie reinforcement. “Y,” “S,” and “R” in the names of the columns stand for “Yin’s spiral”, “Shear critical” and “Rectilinear tie.” “1” and “3” in the names stand for  $0.1f'_cA_g$  and  $0.3f'_cA_g$  axial load. The five-spiral reinforcement is also known as Yin’s spiral because it is first proposed by Yin et al. [12]. The difference in performance between five-spiral and conventional tied columns can be observed by comparing columns Y1S and Y3S to R1S and R3S, respectively. The shear strength of each column was designed to be lower than the flexural strength to ensure that shear failure occurs before flexural failure. The volumetric ratio of transverse reinforcement of all the columns was 0.75% and the area ratio of longitudinal

**Table 1**  
Column design parameters.

Column	Transverse reinforcement	$\frac{P}{f_c A_g}$	Concrete		Transverse reinforcement				Longitudinal reinforcement			
			$f_c$ (MPa)	$f_{ca}$ (MPa)	Bar size @spacing (mm)	$f_{yt}$ (MPa)	$f_{yt}$ (MPa)	$\rho_s$ (%)	Quantity-bar size (mm)	$f_{yt}$ (MPa)	$f_{yt}$ (MPa)	$\rho_g$ (%)
R1S	Rectilinear Tie	0.1	49	48.3	D10@150	420	477	0.75	8-D25 12-D32	420	476	3.84
Y1S	Five-spiral	0.1		48.4	S:D10@135 L:D10@135		477	0.75	8-D25 12-D32		476	3.84
R3S	Rectilinear Tie	0.3		74.6	D10@150		500	0.75	8-D25 12-D32		466	3.84
Y3S	Five-spiral	0.3		76.6	S:D10@135 L:D10@135		443	0.75	8-D25 12-D32		466	3.84

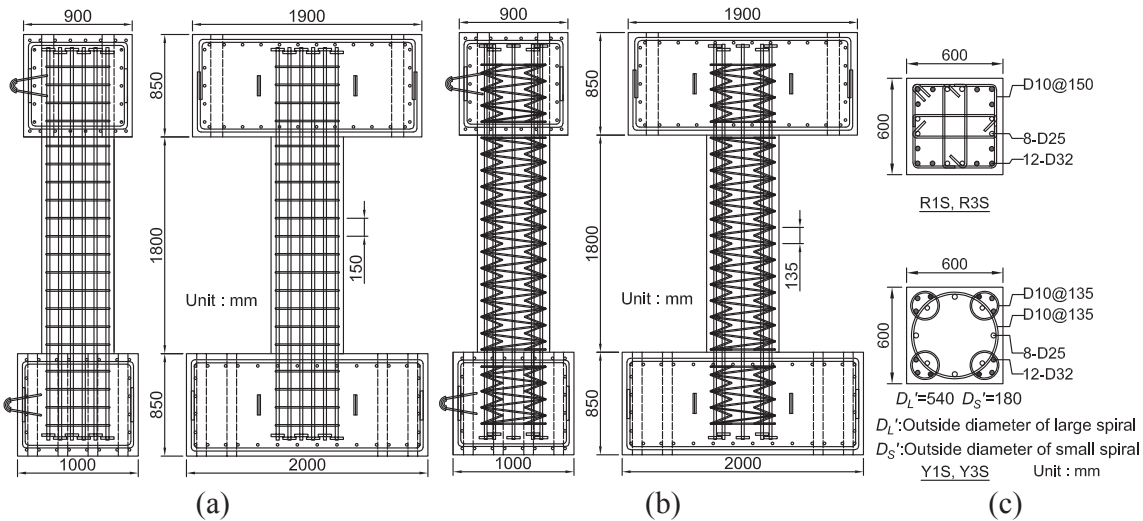


**Fig. 2.** Specimen design: (a) R1S and R3S, (b) Y1S and Y3S, and (c) cross sectional design.

reinforcement was 3.84%. The height and diameter of the columns were 1800 mm and 600 mm, which results in a shear span-to-effective depth ratio of 1.88. The shear span is taken as half of the height because the column was tested in a double curvature fashion. The effective depth is assumed to be 80% of the overall depth of the column cross section. The five-spiral reinforcement contained a large spiral with an outer diameter of 540 mm and four small spirals with an outer diameter of 180 mm. The maximum distance between the inner faces of small and large spirals in the overlapping region was 75 mm, larger than the smaller value of 0.3

times the inner diameter of the small spiral ( $0.3 \cdot 161 = 48$  mm) and 60 mm as required by the reinforced concrete code of Taiwan [16].

The concrete compressive strength was obtained from testing of cylinder specimens with a diameter of 12 cm and height of 24 cm. The specified concrete strength was 49 MPa, which is common for lower story columns in buildings of 10–20 stories in Taiwan. The actual concrete compressive strengths  $f'_{ca}$  of all the columns are listed in Table 1. The ratios of  $f'_{ca}$  to  $f'_c$  of columns with  $0.1f'_c A_g$  axial load (R1S and Y1S) are significantly different from those with  $0.3f'_c A_g$  axial load (R3S and

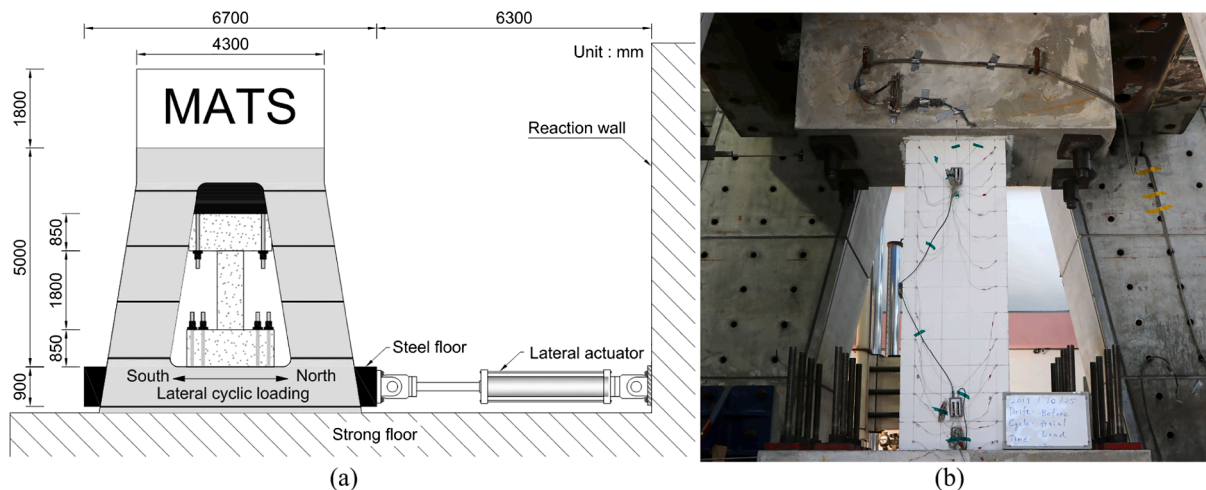


**Fig. 3.** Test setup: (a) MATS and (b) column R3S in MATS.

Y3S) because the concrete of the  $0.1f_cA_g$  columns and that of the  $0.3f_cA_g$  columns were cast in different time by different ready-mix plants. The nominal yield strength of reinforcement was 420 MPa. The actual yield strengths of reinforcement of all the columns are listed in Table 1.

The columns were tested using the Multi-Axial Testing System (MATS) located at the National Center for Research on Earthquake Engineering (NCREE) in Taiwan. The test setup is shown in Fig. 3. The columns were tested in a double-curvature fashion. The top and bottom blocks of each column were fixed to the testing machine. Axial load was applied first and maintained constant throughout the testing. Displacement-controlled lateral cyclic loading was then applied. The loading contained drift ratios of 0.25%, 0.375%, 0.5%, 0.75%, 1.0%, 1.5%, 2.0%, 3.0%, 4.0%, 5.0%, 6.0%. The drift ratio is defined as the relative displacement between the two ends of the column divided by the height of the column (1800 mm). Loading to each drift ratio was repeated three times. The test setup was used to simulate the loading condition of a building column subjected to gravity and seismic loadings. The lateral load versus relative displacement between the two ends of the column were monitored. Moreover, the column deformation was monitored by an optical motion tracking system. The stress responses of reinforcement were monitored using strain gauges that were installed on reinforcement during specimen fabrication.

## 2.2. Damage process and hysteresis behavior

For columns R1S and Y1S, which were subjected to  $0.1f_cA_g$  axial load, flexural and flexural shear cracks started to occur at 0.375% drift near the two ends of the column, which were subjected to higher moments than the other region of the column. At 0.5% drift, web-shear cracks occurred around the middle height of the column. At 0.75% drift, both columns showed long web-shear cracks extending diagonally from the top to the bottom of the column. Moreover, at this drift, R1S showed the peak lateral force for both positive and negative loading directions. Y1S showed the peak lateral force for negative loading direction at this drift but the peak lateral force for positive direction occurred at the next drift level (1%). Fig. 4(a) and (b) show the damage conditions of both columns at 0.75% drift. At 1% drift, both columns started to show spalling of concrete around the corners at the ends of the

column. At 1.5% drift, notable spalling of concrete appeared along diagonal cracks. The extent of spalling increased with the increasing drift. Fig. 4(c) and (d) showed the damage of R1S and Y1S, respectively, at 4% drift, when significant spalling can be observed around the middle height region of the column. Both columns appeared to show similar damage progress until 4% drift. However, the five-spiral reinforcement in Y1S seemed to provide better confinement to core concrete such that even with significant spalling of concrete, a better integrity of core concrete could still be maintained to take the load. As a result, Y1S exhibited a much lower speed of degradation in lateral strength after the peak lateral force. Due to safety concerns, testing of R1S was terminated at 4% while Y1S at 6% when the lateral strength was dropped to 29% and 38%, respectively, of the average peak lateral force (average value of positive and negative responses).

For R3S and Y3S, due to a higher axial load ( $0.3f_cA_g$ ), less flexural cracks appeared at 0.375% drift than R1S and Y1S. At 0.5% drift, web-shear cracks appeared as shown in Fig. 5(a) and (b) for R3S and Y3S, respectively. At this drift, R3S for the negative loading direction and Y3S for both positive and negative loading directions showed the peak lateral force for respective loading direction. R3S for the positive loading direction exhibited the peak lateral force at the next drift level (0.75%). At 1% drift, long diagonal cracks extending diagonally from the top to bottom occurred and spalling of concrete along diagonal cracks started. At 1.5% drift, R3S suddenly showed significant widening of one of the long diagonal cracks, followed by large extent of concrete spalling as shown in Fig. 5(c). The hooks of tie reinforcement were pull out of the core concrete. The column then lost its axial load capacity and hence the testing was terminated. In contrast, at 1.5% drift, spalling of concrete in Y3S was much less than R3S as shown in Fig. 5(d). At the first cycle of 2% drift, Y3S was still able to sustain the axial load. During the second cycle of the loading, the spiral reinforcement broke at several locations, losing its capacity to hold the core concrete together and hence the column lost its axial load capacity. It was evident that the five-spiral reinforcement in Y3S was fully mobilized in providing confinement to core concrete while the tie reinforcement in R3S failed prematurely due to failure of hook anchorage.

Table 2 lists the lateral forces and drift ratios at diagonal cracking and peak lateral load of all the columns. The diagonal cracking is the

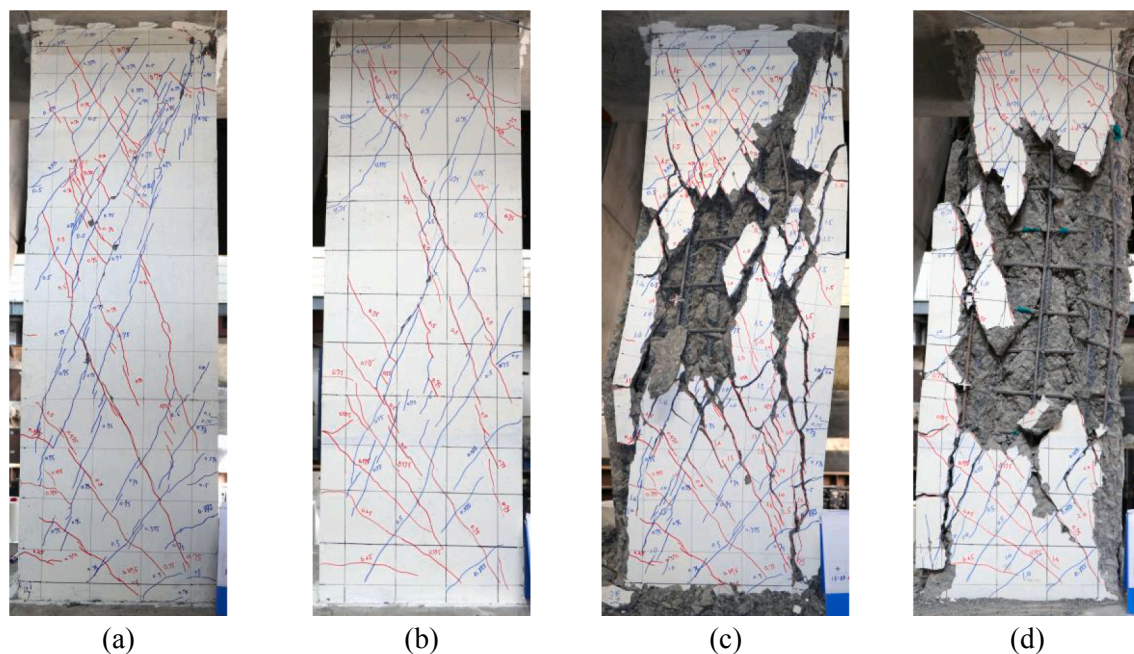


Fig. 4. Damage conditions of columns: (a) R1S at  $-0.75\%$  drift (peak lateral force), (b) Y1S at  $-0.75\%$  drift (peak lateral force), (c) R1S at  $-4\%$  drift, and (d) Y1S at  $-4\%$  drift.

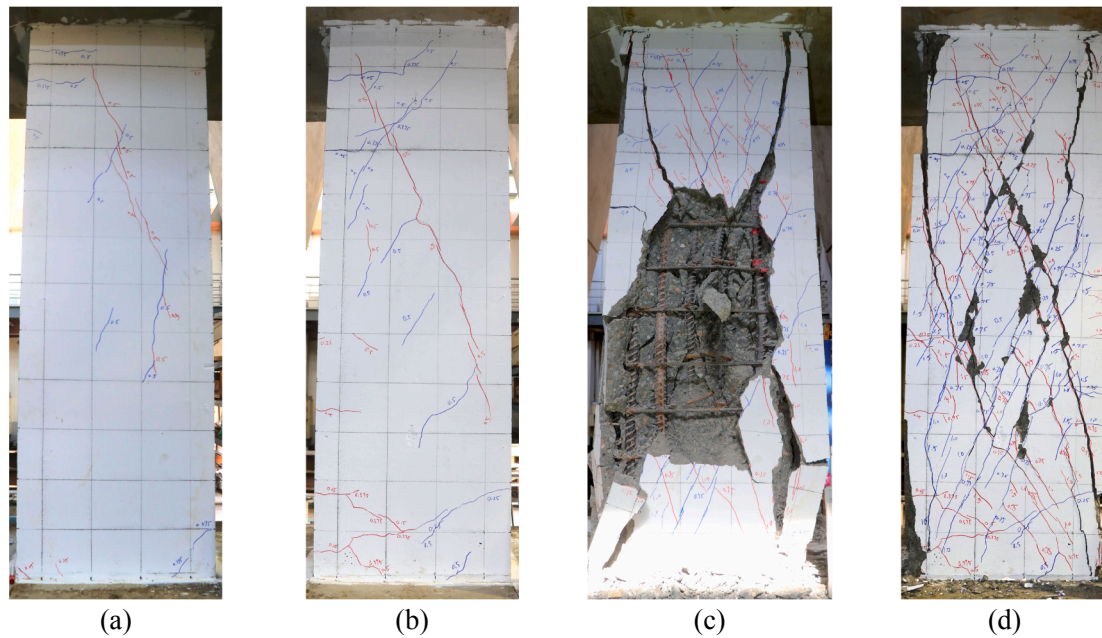


Fig. 5. Damage conditions of columns: (a) R3S at -0.5% drift (peak lateral force), (b) Y3S at -0.5% drift (peak lateral force), (c) R3S at -1.5% drift, and (d) Y3S at -1.5% drift.

Table 2  
Lateral forces and drift ratios at diagonal cracking and peak lateral load.

Column	Diagonal cracking		Peak lateral load			
	Drift ratio (%)	Lateral force (kN)	Positive direction		Negative direction	
			Drift ratio (%)	Lateral force (kN)	Drift ratio (%)	Lateral force (kN)
R1S	0.375%	1247	0.75%	1468	-0.75%	-1333
Y1S	0.375%	1150	1.00%	1381	-0.75%	-1333
R3S	-0.50%	2056	0.75%	2393	-0.50%	-2056
Y3S	0.50%	2218	0.50%	2218	-0.50%	-1976

condition when the first appearance of diagonal cracking that caused significant increase in the stress response of transverse reinforcement. Fig. 6 shows the relationships of the lateral force and drift ratio of all the columns. Fig. 7 shows the envelope responses of the relationships. Note that the P-delta effect due the axial load on the lateral force has been removed. Under an axial load of  $0.1f_c A_g$ , the five-spiral column (Y1S) showed a slightly lower by approximately 3% the peak load (ultimate shear strength) to the counterpart conventional tied column (R1S). However, the five-spiral column showed much slower degradation after the peak load than the tied column. As stated previously, testing of the five-spiral column stopped at 6% drift while that of the tied column stopped earlier at 4%. Both columns could still sustain the axial load when the testing was stopped due to safety concerns. Note that these two columns had the same amount of shear reinforcement. The actual yield strengths of shear reinforcement and actual compressive strengths of concrete of the two columns were similar (Table 1). For the columns subjected to an axial load of  $0.3f_c A_g$ , the five-spiral column (Y3S) showed a slightly lower by approximately 5% the peak load (ultimate shear strength) to the counterpart conventional tied column (R3S). Note that the actual yield strength of shear reinforcement of Y3S was lower than that of R3S (Table 1). However, the five-spiral column showed a larger drift capacity than the tied column. Testing of the five-spiral column was terminated at 2% drift while that of the tied column at 1.5% drift because the axial load could not be maintained as stated previously.

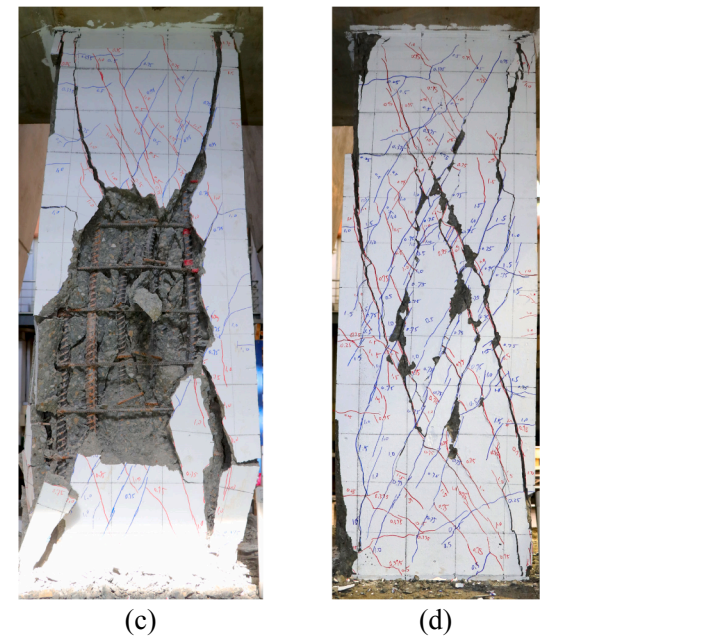


Fig. 8 shows the stress distribution of transverse reinforcement measured at the peak lateral load. Also shown in the figure are the actual yield stresses of transverse reinforcement. It can be seen that all tie reinforcement yielded at the peak lateral load. The large spiral of the five-spiral reinforcement yielded at the peak lateral load for both Y1S and Y3S. The small spiral yielded for Y1S and was very close to yield for Y3S. It appears that the small spirals were effectively interlocked with the large spiral to provide shear resistance to the column.

### 3. Shear strength analysis

#### 3.1. Shear strength model

A shear strength model, referred to as discrete computational shear strength (DCSS) model, has been developed for five-spiral reinforcement in a previous study [18]. The model was developed based on the actual, discrete locations of the interception points between an assumed shear crack and the five spirals. However, the model has not been verified by test data. Moreover, the vertical projection of the assumed crack is equal to the overall depth of the section  $h$  if the crack angle is 45 degrees to the axis of the column. However, the vertical projection is typically taken as  $0.8h$  for columns [17]. In this research, the DCSS model developed by Ou and Ngo [18] is modified so that the vertical projection is equal to  $0.8h$  if the crack angle is 45 degrees to the axis of the column, as illustrated in Fig. 9. The derivation of the modified DCSS model are described as follows and the validation of the model is presented in the next section.

As shown in Fig. 9, a coordinate system is placed on the left side of a column such that the  $x$  axis of the coordinate system passes through the left edge of the large spiral. For the  $i^{\text{th}}$  layer of the  $j^{\text{th}}$  spiral (the colored spiral in Fig. 9), the function of the dotted spiral line (blue line) is

$$y = \frac{s}{2D_j}x + s \left( i - \frac{\ell_j}{2D_j} \right) \quad (1)$$

The function of the solid spiral line (red line) is

$$y = -\frac{s}{2D_j}x + s \left( i + 1 + \frac{\ell_j}{2D_j} \right) \quad (2)$$

A shear crack is assumed to start from a point on the left edge of the

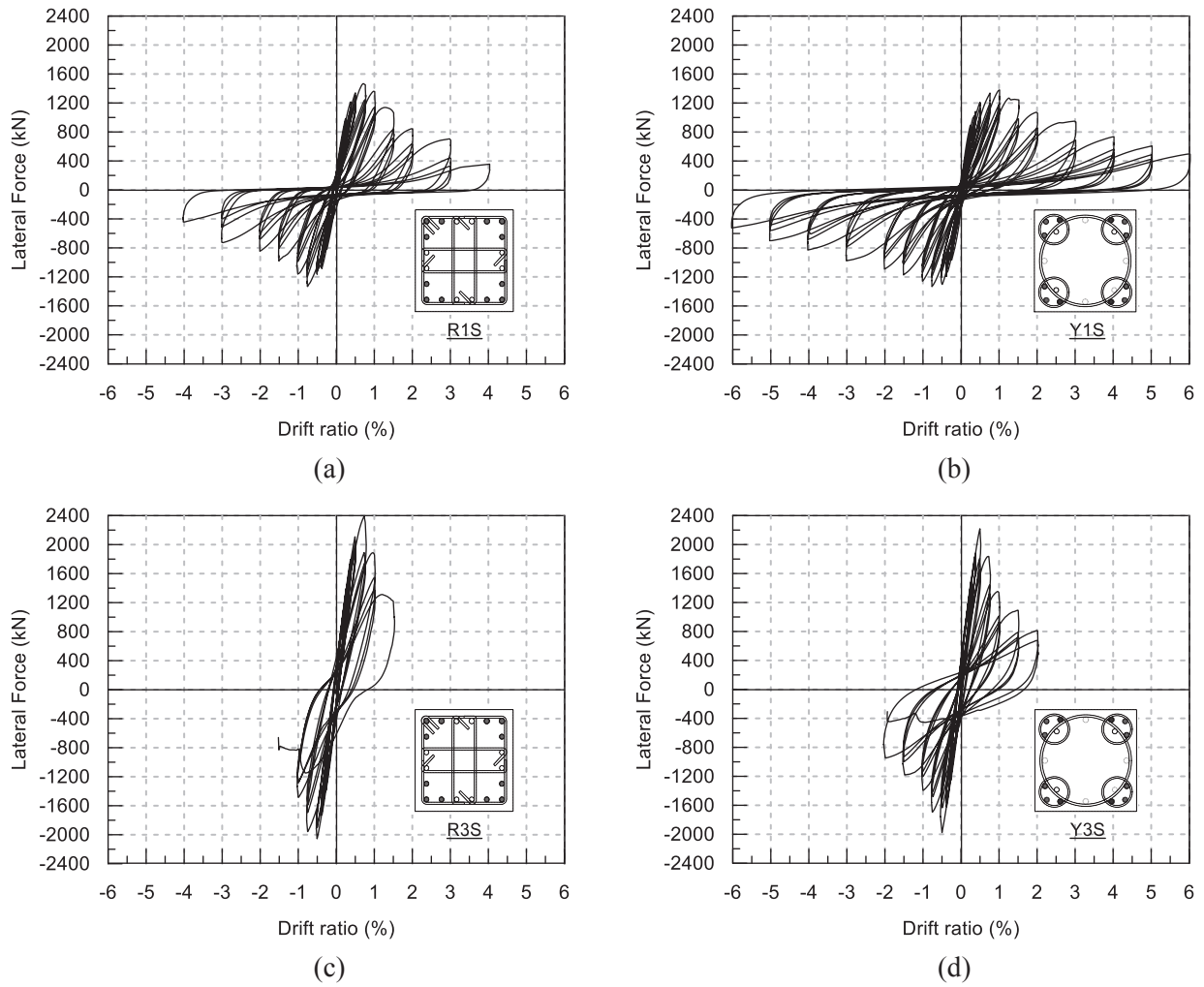


Fig. 6. Hysteretic behavior of columns: (a) R1S, (b) Y1S, (c) R3S, and (d) Y3S.

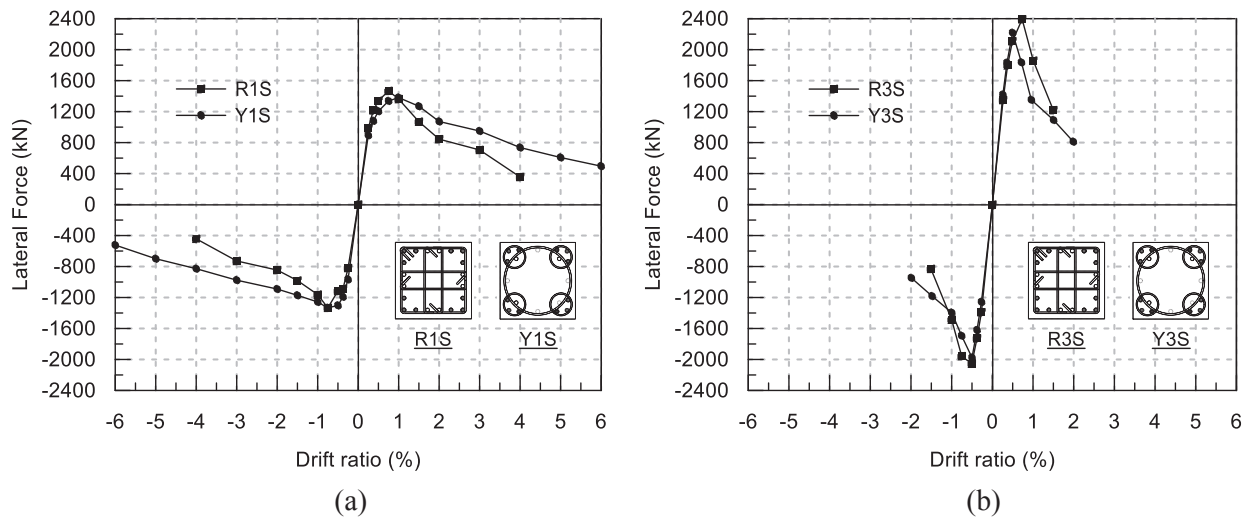


Fig. 7. Envelope responses of columns: (a) R1S and Y1S; (b) R3S and Y3S.

reinforcement as shown in Fig. 9 and propagates for a distance such that the horizontal projection of the crack is 0.8 h. The point on the left edge of the reinforcement where the crack starts is selected so that the extension line of the crack passes through the origin of the coordinate

system. Therefore, the function of the crack is

$$y = xcot\theta \tag{3}$$

The x coordinate of the interception of the dotted spiral line (blue

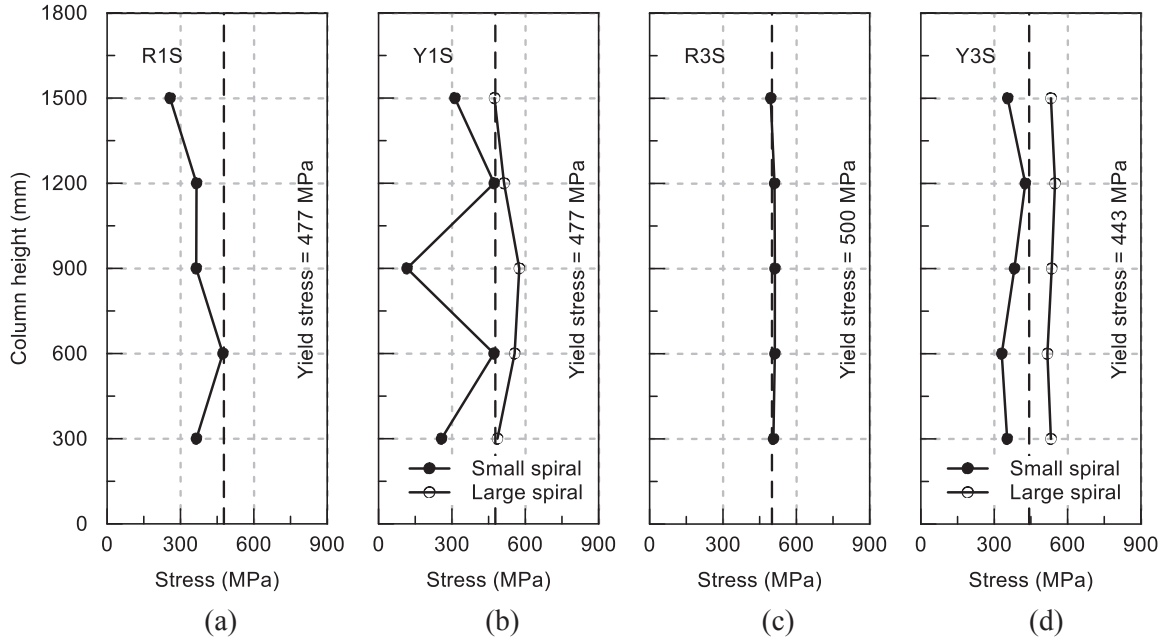


Fig. 8. Stress distribution of shear reinforcement of columns: (a) R1S, (b) Y1S, (c) R3S, and (d) Y3S.

line) and the crack, referred to as  $x_i^1$ , can be obtained by solving Eqs. (1) and (3) for  $x$ .

$$x_i^1 = \frac{s \left( i - \frac{\ell_j}{2D_j} \right)}{\cot\theta - \frac{s}{2D_j}} \quad (4)$$

The range of  $x_i^1$  is limited to the intersection of the boundary of the assumed shear crack, i.e.,  $\ell_c \leq x_i^1 \leq \ell_c + 0.8h$ , and that of the  $j^{\text{th}}$  spiral, i.e.,  $\ell_j \leq x_i^1 \leq \ell_j + D_j$ . A factor  $\phi_b$ , as defined below is used to reflect the fraction of the  $j^{\text{th}}$  spiral that is intersected by the shear crack.

$$\phi_b = \begin{cases} 0 & , \ell_j \geq \ell_c + 0.8h \\ \frac{\ell_c + 0.8h - \ell_j}{D_j} & , \ell_j + D_j \geq \ell_c + 0.8h > \ell_j \\ 1 & , \ell_c + 0.8h > \ell_j + D_j \end{cases} \quad (5)$$

With the  $\phi_b$  factor, the range of  $x_i^1$  can be expressed as  $\ell_j \leq x_i^1 \leq \ell_j + \phi_b D_j$ . The range of  $i$  for  $x_i^1$  can be obtained as below by substituting Eq. (4) for  $x_i^1$  in  $\ell_j \leq x_i^1 \leq \ell_j + \phi_b D_j$ , recognizing  $i$  is an integer.

$$\text{int} \left[ \frac{\ell_j \cot\theta}{s} \right] + 1 \leq i \leq \text{int} \left[ \frac{\phi_b D_j \cot\theta}{s} + \frac{\ell_j \cot\theta}{s} - \frac{\phi_b}{2} \right] \quad (6)$$

The  $\sin\alpha_i^1$  is calculated by the following equation.

$$\sin\alpha_i^1 = \sqrt{1 - \cos\alpha_i^1} = \sqrt{1 - \left( \frac{\ell_j + R_j - x_i^1}{R_j} \right)^2} \quad (7)$$

The  $x$  coordinate of the interception of the solid spiral line (red line) and the crack, referred to as  $x_i^2$ , can be obtained by solving Eqs. (2) and (3) for  $x$ .

$$x_i^2 = \frac{s \left( i + 1 + \frac{\ell_j}{2D_j} \right)}{\cot\theta + \frac{s}{2D_j}} \quad (8)$$

Following a similar derivation as for Eq. (6), the range of  $i$  for  $x_i^2$  can be expressed as the following equation.

$$\text{int} \left[ \frac{\ell_j \cot\theta}{s} \right] \leq i \leq \text{int} \left[ \frac{\phi_b D_j \cot\theta}{s} + \frac{\ell_j \cot\theta}{s} + \frac{\phi_b}{2} - 1 \right] \quad (9)$$

The  $\sin\alpha_i^2$  is calculated by the following equation.

$$\sin\alpha_i^2 = \sqrt{1 - \cos\alpha_i^2} = \sqrt{1 - \left( \frac{\ell_j + R_j - x_i^2}{R_j} \right)^2} \quad (10)$$

The  $\sin\beta_s$  is calculated by the following equation.

$$\sin\beta_s = \frac{1}{\sqrt{1 + \left( \frac{s}{2D_j} \right)^2}} \quad (11)$$

The shear strength of the  $j^{\text{th}}$  spiral  $V_j$  is the summation of all the shear resistances contributed from all the intersection points between the spiral and the shear crack.

$$V_j = \sum_i T_i = \sum_i A_{bfyt} (\sin\alpha_i^1 + \sin\alpha_i^2) \sin\beta_s \quad (12)$$

The shear strength of the five-spiral reinforcement for the assumed shear crack is the summation of all shear resistances of all five spirals.

$$V'_s = \sum_j V_j \quad (13)$$

By moving the location of the shear crack, several values of  $V'_s$  can be obtained. The minimum value is considered as the shear strength of the five-spiral reinforcement and is referred to as  $V_{s,DCSSm}$ .

$$V_{s,DCSSm} = \min(V'_s) \quad (14)$$

Eq. (15) is the equation which the ACI 318 code [17] uses to calculate the shear strength contributed by transverse reinforcement. It is used in this research to calculate the shear strength of tie reinforcement. Moreover, for comparison purpose, Eq. (15) is also used to calculate the shear strength by the five-spiral reinforcement. In the calculation, the contribution from the four small spirals are ignored. The five-spiral reinforcement is conservatively simplified as a single spiral formulated by the central large spiral.

$$V_{s,Code} = \frac{A_v f_{yt} d}{s} \quad (15)$$

The shear strength contributed by concrete  $V_c$  is calculated by Eq. (16), which is from ACI 318 [17] and applied in this research to both five-spiral columns and tied columns.

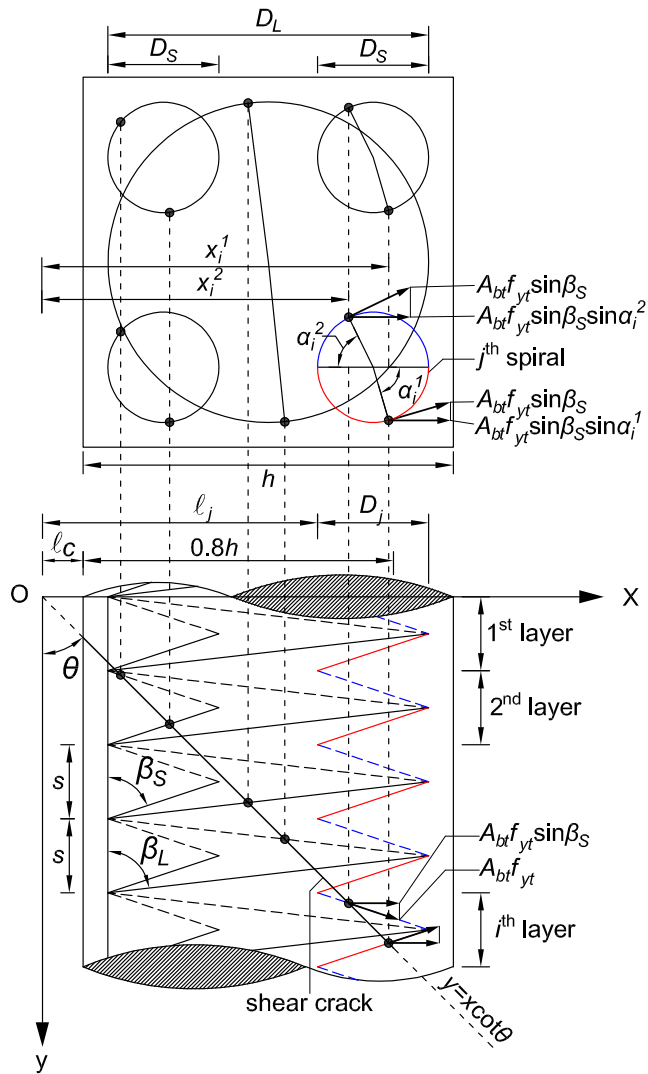


Fig. 9. Modified DCSS model for five-spiral reinforcement.

$$V_c = \left( 0.17\sqrt{f'_c} + \frac{N_u}{6A_g} \right) b_w d \text{ (MPa)} \quad (16)$$

where  $V_c$  should not be taken greater than  $0.42\sqrt{f'_c}b_w d$  and the value of  $N_u/6A_g$  should not be taken greater than  $0.05f'_c$ . The  $d$  is taken as  $0.8h$ .

The shear strength of the column  $V_n$  as defined by Eq. (17) is the summation of the shear strength by concrete  $V_c$  and shear reinforcement  $V_s$ . The  $V_s$  is calculated by Eq. (14) or (15) for five-spiral columns and by Eq. (15) for conventional tied columns.

$$V_n = V_c + V_s \quad (17)$$

Table 3  
Comparison between analysis and test data.

	$V_c$ kN	$V_{s,Code}$ kN	$V_{s,DCSSm}$ kN	$V_{s,DCSS}$ kN	$V_{n,Code}$ kN	$V_{n,DCSSm}$ kN	$V_{n,DCSS}$ kN	$V_{test}$ kN	$M_n$ kN-m	$V_{M_n}$ kN	$\frac{V_{test}}{V_{M_n}}$	$\frac{V_{test}}{V_{n,Code}}$	$\frac{V_{test}}{V_{n,DCSSm}}$	$\frac{V_{test}}{V_{n,DCSS}}$
R1S	565	436	–	–	1001	–	–	1468	1789	1988	0.738	1.466	–	–
Y1S	564	242	331	386	806	895	950	1381	1838	2042	0.676	1.713	1.544	1.454
R3S	1017	457	–	–	1473	–	–	2393	2436	2707	0.884	1.624	–	–
Y3S	1030	225	307	358	1255	1337	1388	2218	2516	2796	0.793	1.768	1.659	1.598

### 3.2. Comparison with test data

The shear strength of all the columns  $V_n$  tested in this research was calculated and listed in Table 3. The  $V_{s,DCSSm}$  and  $V_{s,DCSS}$  in Table 3 respectively represent the shear strength of five-spiral reinforcement calculated by the modified DCSS model developed in this research and the DCSS model developed previously [18]. The crack angle  $\theta$  is set equal to 45 degrees in the calculation. The  $V_c$  of all the columns was calculated by Eq. (16). The  $d$  in Eqs. (15) and (16) is taken as  $0.8h$ . The moment strength of all the columns  $M_n$  was also calculated according to the ACI 318 code [17] and listed in Table 3. Actual material strengths were used in the calculation of  $V_n$  and  $M_n$ .

It can be seen from Table 3 that the peak experimental shear  $V_{test}$  of each column is smaller than the shear corresponding to moment strength  $V_{M_n}$ . The value of  $V_{test}/V_{M_n}$  ranges from 0.676 to 0.884. This means all the columns failed in shear as expected in design. For the shear strength, the calculated shear strength of the five-spiral reinforcement is generally lower than that of the rectilinear tie reinforcement. However, the actual shear strength  $V_{test}$  of the five-spiral columns is only slightly lower than that of rectilinear tie reinforcement. For example, the  $V_{s,DCSSm}$  of Y1S is lower by 24% than the  $V_{s,Code}$  of R1S, but the actual shear strength of Y1S,  $V_{test}$ , is only 6% lower. Note that the transverse reinforcement of Y1S and that of R1S had the same actual yield strength ( $f_{yt}=477$  MPa, Table 1) and the same amount ( $\rho_s = 0.75\%$ , Table 1). The values of  $V_{test}/V_n$  of all columns ( $V_{test}/V_{n,Code}$ ,  $V_{test}/V_{n,DCSSm}$  and  $V_{test}/V_{n,DCSS}$ ) are larger than 1.0, which means the predictions are all conservative. The modified DCSS model produces the values of  $V_{test}/V_{n,DCSSm}$  for five-spiral columns (Y1S and Y3S) very close to the values of  $V_{test}/V_{n,Code}$  for tied columns. The difference is only 4% in average. This finding shows that the modified DCSS model for five-spiral reinforcement provides a degree of conservatism similar to the code equation for the tie reinforcement. The use of the code equation for five-spiral columns by ignoring the contribution of the four small spirals show predictions ( $V_{test}/V_{n,Code}$  for five-spiral columns) that are too conservative than those for tied columns. The DCSS model previously developed show less conservative prediction ( $V_{test}/V_{n,DCSS}$ ) than the modified DCSS model. Note that these findings are based on a limited number of specimens and hence should be used with caution.

### 4. Summaries and conclusions

Large-scale columns with five-spiral reinforcement and those with conventional rectilinear tie reinforcement were tested and compared in this research. Moreover, a discrete computational shear strength (DCSS) model for five-spiral reinforcement was developed and validated by the test results. Important conclusions are summarized as follows.

- (1) All the columns failed in shear as expected in design. With the same amount and similar yield strengths of shear reinforcement and concrete compressive strengths, the five-spiral column under the low axial load (Y1S) showed slightly lower shear strength than the conventional tied columns (R1S). The five-spiral columns under low and high axial loads showed a slower strength degradation after the peak load and hence a larger drift capacity than the counterpart tied columns. Under a high axial load of  $0.3f'_c A_g$ , the five-spiral reinforcement was fully mobilized in

providing shear resistance and confinement to core concrete as evident by fracture of spirals at several locations at the end of test. In contrast, the tie reinforcement failed prematurely due to pullout of hook anchorage.

- (2) A modified DCSS model has been developed in this research for calculating the shear strength of five-spiral reinforcement. In the modified DCSS model, the shear strength is calculated based on actual, discrete locations of the interception points between an assumed shear crack and the five spirals. The location of the assumed shear crack is changed to obtain the minimum shear resistance as the shear strength of five-spiral reinforcement. The modified DCSS model for five-spiral reinforcement combined with the shear strength equation for concrete from the ACI 318 code was found to provide conservative estimate of the shear strength of the five-spiral columns tested. Furthermore, it was found that the degree of conservatism of the modified DCSS model is similar to that of the code equation for the tie reinforcement tested.

#### CRedit authorship contribution statement

**Yu-Chen Ou:** Conceptualization, Methodology, Writing - original draft. **Jhe-Yan Li:** Data curation, Visualization. **Hwasung Roh:** Conceptualization, Writing - review & editing.

#### Declaration of Competing Interest

The authors declare that they have no known competing financial interests or personal relationships that could have appeared to influence the work reported in this paper.

#### Acknowledgements

The authors would like to thank the financial support from the Ministry of Science and Technology of Taiwan under Contract Nos. 107-2923-E-002 -004 -MY2 and from the National Center for Research on Earthquake Engineering (NCREE) of Taiwan. In addition, this research was partially supported by the Basic Science Research Program through the National Research Foundation of Korea (NRF) funded by the Ministry of Education (Grant No. 2018R1D1A1B07048759).

#### References

- [1] Murphy, L.M. (Scientific Coordinator). San Fernando, California, Earthquake of February 9, 1971. National Oceanic and Atmospheric Administration, U.S. Department of Commerce, Washington, D.C., Volume I. Effects on building structures; 1973. p. 841.
- [2] Mlakar PF, Dusenberry DO, Harris JR, Haynes G, Phan LT, Sozen MA. Description of structural damage caused by the terrorist attack on the Pentagon. *J Perform Constr Facil* 2005;19(3):197–205.
- [3] Tanaka H, Park R. Seismic design and behavior of reinforced concrete columns with interlocking spirals. *ACI Struct J* 1993;90(2):192–203.
- [4] McLean DI, Buckingham GC. Seismic performance of bridge columns with interlocking spiral reinforcement, report no. WA-RD 357.1. Washington, USA: Washington State Transportation Center; 1994.
- [5] Otaki T, Kuroiwa T. Test of bridge columns with interlocking spiral reinforcement and conventional rectangular hoop with ties. Reports of the Technological Research Institute, Tokyo Construction Co.Ltd, Japan, No. 25; 1999. p. 33–38.
- [6] Shito K, Igase Y, Mizugami Y, Ohasi G, Miyagi T, Kuroiwa T. Seismic performance of bridge columns with interlocking spiral/hoop reinforcements. Osaka, Japan: First fib Congress; 2002.
- [7] Kawashima K. Enhancement of flexural ductility of reinforced concrete bridge columns. In: First international conference on urban earthquake engineering, Tokyo Institute of Technology, Tokyo, Japan; 2004. p. 85–95.
- [8] Correal JF, Saiidi MS, Sanders D, El-Azazy S. Shake table studies of bridge columns with double interlocking spirals. *ACI Struct J* 2007;104(4):393–401.
- [9] Ou YC, Ngo SH, Yin SY, Wang JC, Wang PH. Shear behavior of oblong bridge columns with innovative seven-spiral transverse reinforcement. *ACI Struct J* 2014; 111(6):1339–49.
- [10] Ou YC, Ngo SH, Roh H, Yin SY, Wang JC, Wang PH. Seismic performance of concrete columns with innovative seven- and eleven-spiral reinforcement. *ACI Struct J* 2015;112(5):579–92.
- [11] Ou YC, Ngo SH. Discrete shear strength of two- and seven-circular-hoop and spiral transverse reinforcement. *ACI Struct J* 2016;113(2):227–38.
- [12] Yin SYL, Wu TL, Liu TC, Sheikh SA, Wang R. Interlocking spiral confinement for rectangular columns. *ACI Concrete Int* 2011;33(12):38–45.
- [13] Yin SYL, Wang JC, Wang PH. Development of multi-spiral confinements in rectangular columns for construction automation. *J Chin Inst Eng* 2012;35(3): 309–20.
- [14] Wu TL, Ou YC, Yin YL, Wang JC, Wang PH, Ngo HS. Behavior of oblong and rectangular bridge columns with conventional tie and multi-spiral transverse reinforcement under combined axial and flexural loading. *J Chin Inst Eng* 2013;36 (8):980–93.
- [15] Kuo MT. Axial compression tests and optimization study of 5-spiral rectangular rc columns. Master Thesis. Taiwan: National Chiao Tung University; 2008.
- [16] CPAMI. Design specifications for reinforced concrete structures. Taiwan: Construction and Planning Agency, Ministry of the Interior; 2019.
- [17] ACI Committee 318. ACI 318-19 building code requirements for structural concrete (ACI 318-19) and commentary (ACI 318R-19). American Concrete Institute; 2019.
- [18] Ou YC, Ngo SH. Discrete computational shear strength models for five- six- and eleven-circular-hoop and spiral transverse reinforcement. *Adv Struct Eng* 2016;19 (1):23–37.